

1/F NOISE, THE MEASUREMENT OF TIME AND NUMBER THEORY

MICHEL PLANAT

*Laboratoire de Physique et Métrologie des Oscillateurs du CNRS
32 Avenue de l'Observatoire, 25044 Besançon Cedex, France*

Received (received date)

Revised (revised date)

Accepted (accepted date)

Time and frequency measurements of a high frequency oscillator need the comparison to a reference oscillator: the physical units of the measurement are the integers and the relevant approach is analytical number theory. We show this in the context of the moon-sun calendar discovered in ancient Greece and in the context of a communication receiver. It is shown that the resets in time measurements are governed by continued fraction expansions and that their low frequency statistics connects to prime number theory. A link between Riemann hypothesis and $1/F$ noise arises in this context.

Keywords: 1/F Noise, Prime Number Theory, Oscillators, Electronics.

1. The Time and Noise in Oscillators

Over the last years it has been observed that low frequency noise of electronic oscillators carries a strong arithmetical structure [1], [2], [3]. Such a structure was implicitly discovered by the Greeks when establishing their moon-sun calendars. Time and noise go hand by hand in the astronomical calendar and in the superheterodyne receiver discovered by E.H. Armstrong at the dawn of the electronic age [4].

In the Greek calendar one divides the tropical year by the moon year in units of the earth day and one gets 12 (the number of months in a sun year), plus $\frac{1}{2}$, or $\frac{1}{3}$ or $\frac{3}{8}$ depending on the approximation of the ratio by rational numbers: this can be taken into account by adding one month every two years, or one month every three years or three months every eight years respectively.

The random reset of a time period takes place automatically in Armstrong's superheterodyne detection which is based on mixing of two input oscillators and baseband filtering [2]. This principle has wide applicability in most communication receivers. We found that as a result the mean period fluctuates with $1/F$ power spectral density. The mathematical structure underlying the resets in the Greek

calendar and in Armstrong's receiver is continued fraction expansions of the period ratio between the oscillators. This also resorts to the general theory of primes.

In Sect. 2 we remind some properties of continued fractions for the pedestrian in the context of the moon-sun calendar. The arithmetical structure of the mixer+filter set-up is described in Sect. 3. Finally Sect. 4 is an attempt to connect the observed randomness of frequency resets to prime number theory.

2. The Moon-Sun calendar

Most early calendars have been devised from the motion of moon and sun as observed from the earth. In the astronomical calendar one finds 365.242191 days for the tropical year (equinox to equinox) and 29.530589 days for the moon year (new moon to new moon). The ratio is $\nu = 12.4952 \simeq 12$ months $\frac{1}{2}$. Moon-sun calendars are all based on a principle which was recognized in the 18th century by Laplace: continued fractions. The continued fraction expansion of the ratio ν between the sun year and the moon year is

$$\nu = \frac{365.242191}{29.530589} = 12 + \frac{1}{2 + \frac{1}{1 + \frac{1}{2 + \frac{1}{1 + \frac{1}{1 + \frac{1}{17 + \dots}}}}}} \quad (1)$$

The rule is quite simple [5]: one takes the integer part $a_0 = [\nu] = 12$ of the real number ν and its fractional part $\nu_1 = \nu - [\nu] \simeq 0.368$; then one takes the inverse $1/\nu_1 \simeq 2.715$, its integer part $a_1 = [1/\nu_1] = 2$ and its fractional part $\nu_2 = 1/\nu_1 - a_1 \simeq 0.715$; one takes the inverse of the new number $1/\nu_2 \simeq 1.398$, its integer part is $a_2 = [1/\nu_2] = 1$ and its fractional part is $\nu_3 = 1/\nu_2 - a_2 \simeq 0.398$; and so on : $1/\nu_3 \simeq 2.514$, $a_3 = [1/\nu_3] = 2$, $\nu_4 = 1/\nu_3 - a_3 \simeq 0.514$. Formally

$$\nu = \{a_0; a_1, a_2, \dots, a_i, a_{i+1}, \dots\} \quad (2)$$

where the series of integer parts (the so-called partial quotients) is set on the same line to simplify the writing.

A moon-sun calendar is implicitly based on the use of the continued fraction (1): one chooses a year with 12 months and one corrects by taking into account new terms in the expansion. The first approximation is not precise since 12 moon months lead to $12 \times 29.53 \simeq 354$ days for the sun year. If one corrects to first order one adds $\frac{1}{2}$ to 12, that is one month every two years: the year now has $12.5 \times 29.53 \simeq 369$ days. To second order the correction is $\frac{1}{2+1/1} = \frac{1}{3}$, that is one adds one month every 3 years, the year now has $12.333 \times 29.53 \simeq 364$ days. To third order the correction is $\frac{1}{2+1/(1+1/2)} = \frac{1}{2+2/3} = \frac{3}{8}$, that is one adds 3 months every 8 years leading to a year with $12.375 \times 29.53 \simeq 365$ days. This last correction was finally taken by the Greeks as the octaeterid. The metonic cycle which adds

two new terms in the continued fraction was also found but not implemented by the Greeks

$$\nu = \{12; 2, 1, 2, 1, 1\} = 12 + \frac{7}{19} = \frac{235}{19} \quad (3)$$

It adds 7 months every 19 years and the year now has 365.246 days which is close to the exact value 365.242 days.

Continued fractions find applications in many fields. The ratio

$$\nu_{\text{gold}} = \frac{1 + \sqrt{5}}{2} = \{1; 1, 1, 1, \dots\} = \{1, \bar{1}\} \quad (4)$$

was recognized in many civilisations and used by the architect Le Corbusier. Similarly the number

$$\nu_{\text{silver}} = 1 + \sqrt{2} = \{1, \bar{2}\} \quad (5)$$

is approximately the size ratio for the A4 format, that is $\frac{29.7}{21} \simeq \frac{99}{70} = \{1; 2, 2, 2, 2\}$.

Examples can be found in transcendental numbers, that is numbers which are not solutions of an algebraic equation (a polynomial with integer coefficients), such as

$$\pi = \{3; 7, 15, 1, 292, 1, 1, 1, 2, 1, 3, 1, 14, 2, 1, 1, 2, 2, 2, 1, 84, 2, \dots\} \quad (6)$$

for which the approximation $\pi \simeq \{3; 7\} = \frac{22}{7}$ is well known. Lagrange proved that the necessary and sufficient condition for a continued fraction to be periodic is for ν to be a quadratic irrational number. But the transcendence of π (and the impossibility of circle quadrature) was only proved in 1882 by Lindemann.

3. The Superheterodyne Calendar

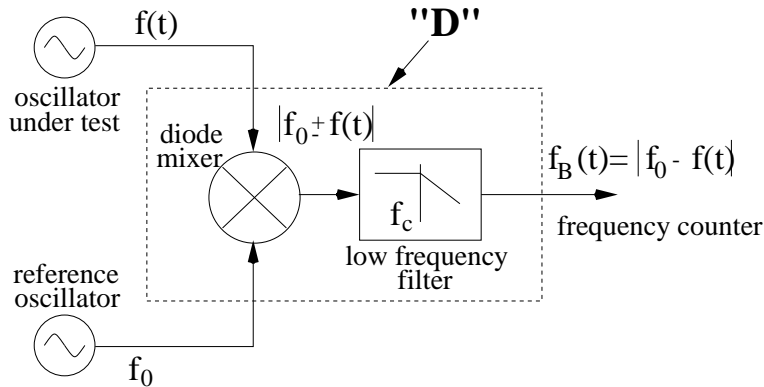


Fig 1. Schematic of the superheterodyne detector "D".

In Armstrong's receiver a reference oscillator, of frequency f_0 , is compared to a test oscillator of frequency $f(t)$ thanks to a nonlinear element. In our measurements the mixer element is a double balanced mixer with four Schottky diodes [2]. A low frequency filter is used to remove high frequencies so that only frequencies close to

baseband remain. At the output of the detector “**D**” one observes the difference between the frequencies of input oscillators

$$f_B(t) = |f_0 - f(t)| \quad (7)$$

If the input frequencies are close to each other the beat frequency is very low and as a result the detector shows a great sensitivity $k = \frac{f_B}{f}$ with a relative frequency error given as

$$y = \frac{\delta f(t)}{f(t)} = \frac{\delta f_B(t)}{f_B} \times \frac{f_B}{f} \quad (8)$$

Let us choose input frequencies $f_0 \simeq f = 10$ MHz, and a beat frequency $f_B = 1$ Hz and let us assume that one observes the relative frequency fluctuation $\frac{\delta f_B}{f_B} = 10^{-6}$, the relative frequency fluctuation of the oscillator under test is

$$y = \frac{\delta f_B}{f_B} \times \frac{1}{k} = 10^{-6} \times 10^{-7} = 10^{-13} \quad (9)$$

a very small number, which is equivalent to jumping one period every 10^{13} periods. Now a millenium equals $3600 \times 24 \times 30 \times 12 \times 100 = 3 \times 10^{10}$ sec; in other words the precision (9) is equivalent to loose 1 msec over three millenia. It is however equivalent to the precision achieved in a good quartz crystal oscillator.

Until now we neglected harmonic interactions in the mixing process. In addition to the fundamental beat frequency $f_B = |f_0 - f(t)|$ there are harmonic beats such as $f_B = |3f_0 - 5f(t)|$. At each rational number $\nu = \frac{p}{q}$, there may be a basin made of two straight lines of slope q (see Fig. 2). To understand this, one should remind that there is a filter of cut-off frequency f_C at the output of the mixer so that

$$f_B = |pf_0 - qf(t)| \leq f_c \quad (10)$$

In the application to demodulation in a communication receiver, the frequency of one channel is f . However due to intermodulation frequencies as given in (10), there are many channel frequencies $f = (pf_0 \pm f_B)/q$ for a given intermediate frequency f_B instead of one. The unwanted signals have to be rejected using sophisticated architectures or highly selective filters [4].

Performing this task using sophisticated electronics does not solve the problem of understanding the nonlinear dynamics of the detector. I reproduce here part of the comments of one referee of this paper

“The basic idea of the superheterodyne receiver is to select a channel by converting the input signal into an intermediate frequency f_B , amplifying and filtering, and then detecting the converted signal. The upper and lower sidebands remain separated in the conversion, and are overlapped in the detection process. On the other hand, the scheme in Fig. 1, in the described conditions, works as a superheterodyne receiver without detector, despite the low pass filter and the word detector used in the caption. . .

This makes me think to a synchrodyne scheme, in which conversion and detection are performed in a single operation. I wish to stress that I take the word detection as it is used in the field of wireless engineering. Accordingly, detecting means that

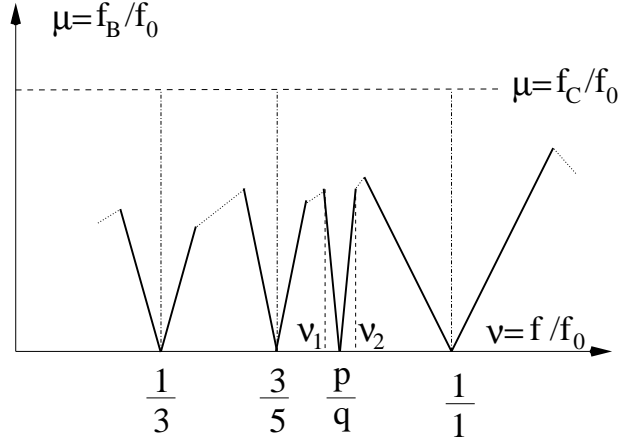


Fig 2. The intermodulation spectrum in detector “D”.

the radiofrequency signal is down converted to baseband, and therefore the lower sideband folded into positive frequencies”

Equation (10) may be rewritten by using the ratio $\nu = \frac{f(t)}{f_0}$ between the two oscillators at the input of “D”

$$\left| \nu - \frac{p}{q} \right| \leq \frac{f_c}{q f_0} \quad (11)$$

or by using the relative error $\mu = \frac{f_B}{f_0}$

$$\mu = \frac{f_B}{f_0} \leq \frac{f_c}{f_0} \quad (12)$$

Equation (12) implies that the result of the measurement is located below the dotted line at $\mu = \frac{f_c}{f_0}$, but it still doesn’t explain the observed basins.

From now we postulate that the detector “D” operates like a moon-sun calendar by truncating the continued fraction (2) according to the cut-off frequency f_c . Like the calendar it performs jumps to correct the errors. These jumps are the underlying structure of $1/F$ noise, which is the universal feature of all rythmic systems [2]. Let us compare relation (11) to the following well known property of continued fractions expansions [1], [5]

$$\left| \nu - \frac{p_i}{q_i} \right| \leq \frac{1}{a_{i+1} q_i^2} \quad (13)$$

Fraction $\frac{p_i}{q_i} = \{a_0; a_1, a_2, \dots, a_i\}$, which is a so-called convergent, means that the continued fraction expansion is truncated at level i and a_{i+1} is the first neglected partial quotient. The relation (13) is the resulting error. The shift is different in decimal approximations $\frac{a_i}{b_i}$ for which one gets

$$\left| \nu - \frac{a_i}{b_i} \right| \leq \frac{1}{b_i} \quad (14)$$

As an example for $\pi \simeq 3.14159$, $\frac{a_1}{b_1} = 3$, $\frac{a_2}{b_2} = \frac{31}{10}$, $\frac{a_3}{b_3} = \frac{314}{100} \dots$ satisfy (14), while the first diophantine approximations of π are $\frac{p_1}{q_1} = 3$, $\frac{p_2}{q_2} = \frac{22}{7}$, $\frac{p_3}{q_3} = \frac{333}{106}, \dots$ and satisfy (13). Diophantine approximation is better than decimal approximation for π since there are large terms in the continued fraction expansion; this is in contrast to numbers ν_{gold} et ν_{silver} in (4) and (5) where the continued fraction expansion only shows small partial quotients 1 and 2.

From the filtering condition (11) and the diophantine condition (13) we expect that the detector “D” will truncate at

$$a_{i+1} = a_{\max} = \left[\frac{f_0}{f_c q_i} \right] \quad (15)$$

where $[]$ means the integer part. Eq. (15) can be proved rigorously and is in very good agreement with all experiments on receiver “D” [2], [6]. In addition, since $a_{\max} > 1$, we get $q_i \leq q_{\max} = \frac{f_0}{f_c}$. For example if one chooses $f_0 = 10$ MHz and $f_c = 300$ kHz, $q_{\max} = 33$, the fundamental basin $\frac{p_i}{q_i} = \frac{1}{1}$ where $q_i = 1$ will be truncated at $a_{\max} = \left[\frac{10}{0.30} \right] = 33$, and the basin of $\frac{p_i}{q_i} = \frac{3}{5}$ will be truncated at $a_{\max} = \left[\frac{10}{0.30 \times 5} \right] = 6$. The frequency structure of “D” now condensates into a single equation which collects (11), (13) and (15)

$$\left| \nu - \frac{p_i}{q_i} \right| \leq \frac{f_c}{f_0 q_i} \quad (16)$$

where we remind that the $\frac{p_i}{q_i}$ are the convergents, that is the truncations of the continued fraction expansions of ν . This is illustrated in Fig. 3.

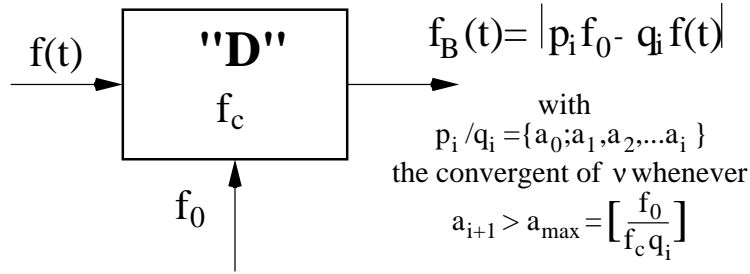


Fig 3. Detector “D” is a diophantine approximator.

We expect the spectrum in Fig. 2 to be built with straight lines of slope q_i emanating from the points $\frac{p_i}{q_i}$. It is easy to show [2], [3] that the edges of the basins are located at

$$\begin{aligned} \nu_1 &= \{a_0; a_1, a_2, \dots, a_i, a_{\max}\} \\ \nu_2 &= \{a_0; a_1, a_2, \dots, a_i - 1, 1, a_{\max}\} \end{aligned} \quad (17)$$

where the partial quotients before a_{\max} corresponds to the two possible expansions of the rational number $\frac{p_i}{q_i}$. The basin of number $\nu = \frac{3}{5} = \{0; 1, 1, 2\}$ extends to

$\nu_1 = \{0; 1, 1, 2, a_{\max}\}$, $\nu_2 = \{0; 1, 1, 1, 1, a_{\max}\}$. With $a_{\max} = 6$ as above one finds $\nu_1 = \frac{19}{32} \simeq 0.594$ et $\nu_2 = \frac{21}{34} \simeq 0.618$. For a reference oscillator with $f_0 = 10$ MHz, this corresponds to a frequency bandwidth $(0.618 - 0.594) \times 10^7$ MHz = 240 kHz.

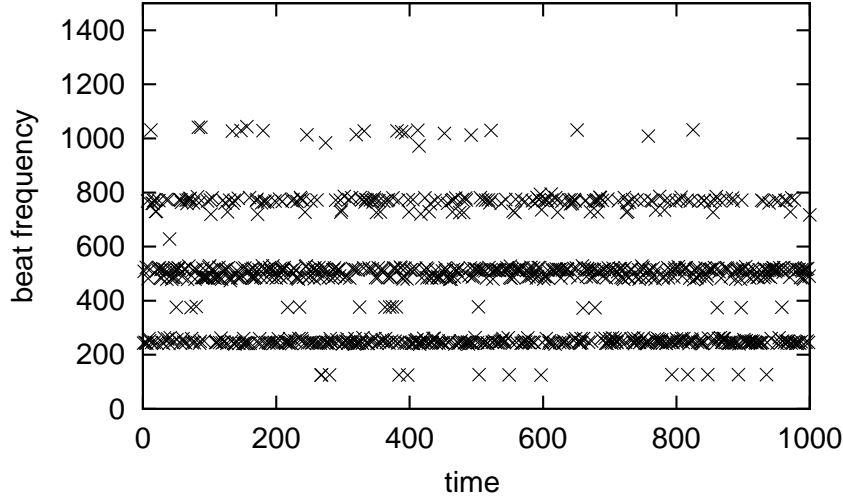


Fig 4. Frequency jumps (in Hz) in the superheterodyne detector. Input frequencies are $f_0 = 1.000\,000\,07$ MHz and $f = 0.599\,975$ MHz. The unit of time is the integration time 1 msec.

It is remarkable that a detailed understanding of the dynamics of frequencies may be obtained without resort to amplitudes. The nonlinearity inherent in the mixing process is such that each harmonic has its own amplitude. This may be also described from analytical rules as it is stressed in [2] and briefly evoked after Eq. (25). Accordingly the amplitude of each harmonic follows from the understanding of the Farey tree as it is related to the Franel-Landau formulation of Riemann hypothesis (see Sect. 4 for details).

Let us remind that our first goal is to characterize the oscillator under test of fluctuating frequency $f(t)$. So the working point slightly fluctuates in the selected basin. In our experiment of Fig. 4 we chose $\frac{p_i}{q_i} = \frac{3}{5}$, with the input reference frequency $f_0 = 1.000\,000\,07$ MHz and oscillator under test frequency $f = 0.599\,975$ MHz. This corresponds to the ratio $\nu = \frac{f}{f_0} = 0.599\,974\,958\dots = \{0; 1, 1, 2, 1596, 1, 10\dots\}$. This is very close to a resonance such as

$$\nu(a) = \{a_0; a_1, a_2, \dots, a_i, a\} = \frac{p(a)}{q(a)} \quad , a > a_{\max} \quad (18)$$

Here we performed contiguous measurements and it was found on Fig. 4 that the observed frequencies are those predicted from the following relation

$$f_B = |p(a) f_0 - q(a) f| \quad \text{with } 1589 \leq a \leq 1605 \quad (19)$$

The detector jumps randomly from one value to the other. For example for $a = 1598, 1599, 1600$ we have $f_B = 135$ Hz, 261 Hz and 386 Hz respectively and for

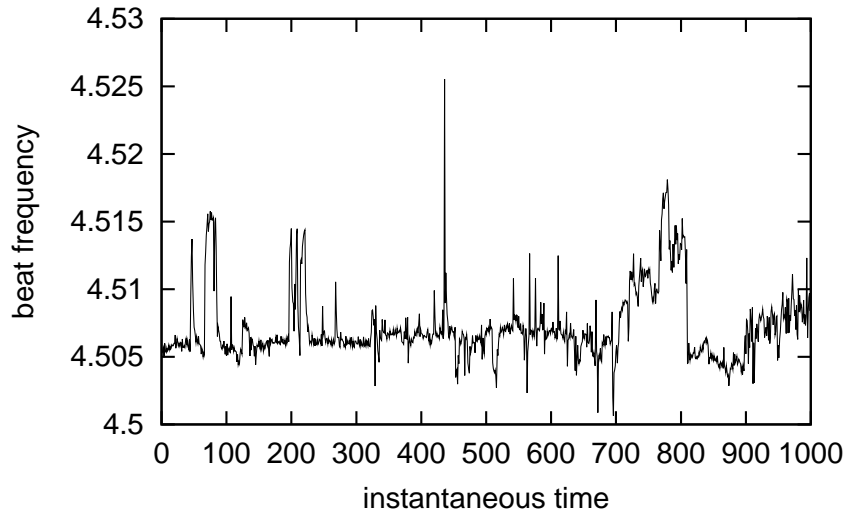


Fig 5. Instantaneous beat frequency (in Hz) for beat frequency close to baseband. Input frequencies are $f \sim f_0 \sim 5.0206$ MHz. The unit of time is the period.

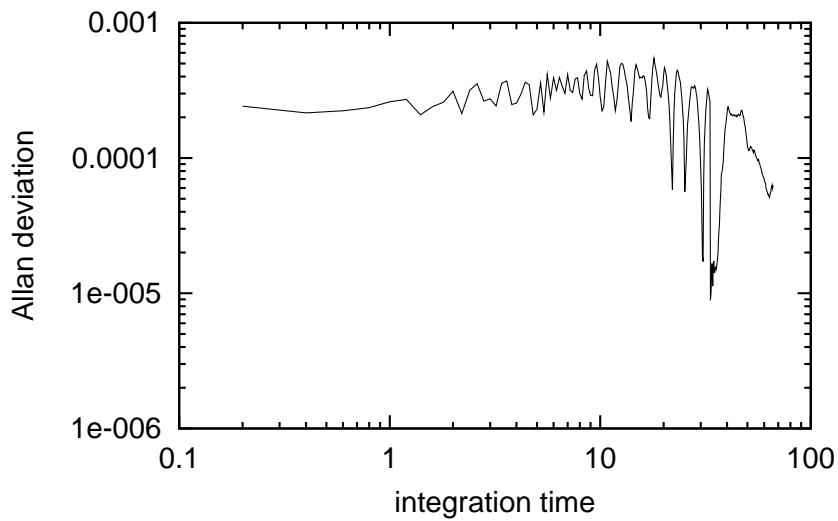


Fig 6. Allan deviation for the file plotted in Fig. 5 (beat frequency close to baseband). The integration time is in sec.

$a = 1593, 1594, 1595$ we have $f_B = 490$ Hz, 365 Hz, and 240 Hz. The range of observed values of f_B is restricted to the bandwidth of counting measurement: it is defined as the inverse of the integration time τ . Here we used $\tau = 1$ ms so that $f_B \leq 1$ kHz.

As in the moon-sun calendar these jumps have the aim to correct the errors that the detector encounters in its read-out of time.

For experiments performed very close to baseband $f_B \simeq 0$ there are many allowed values of index a and it is difficult to identify which basin is occupied at a given time. An example is given in Fig. 5. Here we used input oscillators at frequencies $f \sim f_0 \sim 5.0206$ MHz and a beat frequency $f_B \sim 4.5$ Hz. The statistics may be defined from the Allan deviation $\sigma_y(\tau)$ which is the mean squared value of the relative frequency deviation between adjacent samples

$$\sigma_y^2(\tau) = \frac{1}{2} \langle (y_{l+1}(\tau) - y_l(\tau))^2 \rangle \quad (20)$$

where $y_l(\tau) = \frac{f_B^{(l)}(\tau)}{f_B}$ is the relative beat frequency for the measurement l over the integration time τ , the index $l = (1, 2, \dots, N)$ stands for the N measurements and $\langle \rangle$ means the averaging.

The observed Allan deviation in Fig. 6 is almost constant and this corresponds to a $1/F$ frequency noise.

4. The Statistics of Frequency Jumps and Prime Number Theory

We found in Sect. 3 that the measurement of time in an oscillator involves continued fractions, but we still didn't discover which statistics governs random frequency jumps in time. One tentative arithmetical program for the phase of jumps is

$$\begin{array}{l} n: \quad 1 \quad 2 \quad 3 \quad 4 \quad 5 \quad 6 \quad 7 \quad 8 \quad 9 \quad 10 \quad 11 \quad 12 \dots \\ \mu(n): \quad 1 \quad -1 \quad -1 \quad 0 \quad -1 \quad 1 \quad -1 \quad 0 \quad 0 \quad 1 \quad -1 \quad 0 \dots \end{array}$$

where the program $\mu(n)$ is the so-called Möbius function

$$\mu(n) = \begin{cases} 1 & \text{for } n = 1 \\ 0 & \text{if } n \text{ is divisible by a square} \\ (-1)^k & \text{if } n \text{ is the product of } k \text{ distinct prime numbers} \end{cases} \quad (21)$$

Every integer number may be decomposed into a product of powers of distinct prime numbers so that it is easy to calculate Möbius function. Examples are $n = 12 = 3 \times 2^2$ for which we get $\mu(12) = 0$; for $n = 11$, $k=1$ and $\mu(11) = -1$ and for $t = 6 = 3 \times 2$, $k = 2$ and $\mu(6) = 1$.

Möbius function $\mu(n)$ looks random. However it carries a very important multiplicativity property $\mu(mn) = \mu(m)\mu(n)$ if $(m, n) = 1$ and $\mu(mn) = 0$ otherwise, that is for instants which are prime to each other, the phase jump at time mn is the product of phase jumps at preceding times m et n .

One can ask whether the cumulated phase $M(t)$ (see Fig. 7) is of the brownian motion type. The answer is almost yes, since one expects

$$M(t) = \sum_{n=1}^{n=t} \mu(n) = O(t^{\frac{1}{2}+\epsilon}), \quad \text{whatever } \epsilon \quad (22)$$

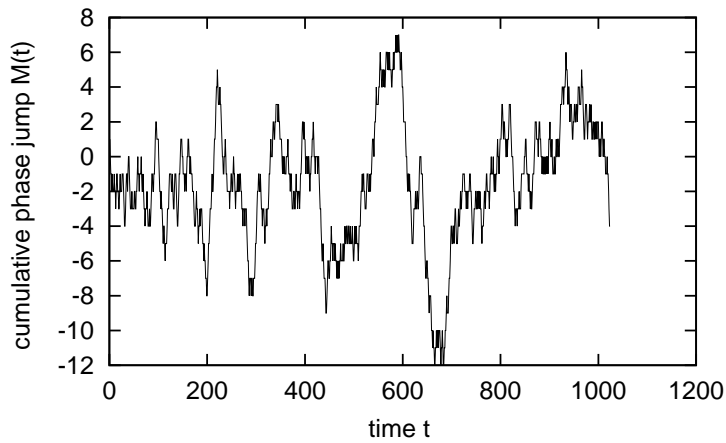


Fig 7. Cumulated phase for the Möbius jumps

where the symbol $O(t^{\frac{1}{2}+\epsilon})$ means that the shift from the initial position is a bit faster than \sqrt{t} , whatever the non zero constant ϵ .

In 1897 Mertens conjectured that $\epsilon = 0$, but this was disproved in 1984 by Odlyzko for very large numbers t . The largest number in physics doesn't exceed 10^{80} , the number of particles in the whole universe, so that taking $\epsilon = 0$ should have no obvious consequence in a physical experiment. The hypothesis that (22) holds for $\epsilon \neq 0$ is of great mathematical significance. Computation of $\mu(n)$ needs the decomposition of n into powers of prime factors, so that the property (22) is a general property of prime numbers. It is one formulation of the so-called "Riemann hypothesis". It underlies many mathematical theorems but it is still unproved. A one million dollars prize is promised by Clay Mathematics Institute in Cambridge, Massachusetts, for its proof (see http://www.claymath.org/prize_problems).

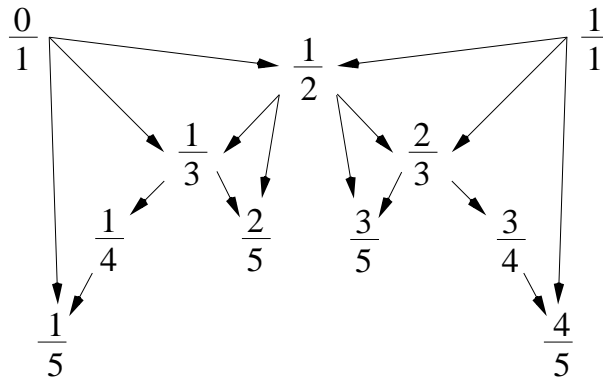


Fig 8. The Farey tree

Möbius function as a program for phase jumps was chosen for its connection to the problem of superheterodyne detection. It is observed in Fig. 2 that the largest

basins correspond to irreducible fractions $\frac{p_i}{q_i}$ with small denominator

$$q_i \leq t \tag{23}$$

These fractions are the convergents at level i in (2); they can be ordered as a so-called Farey tree. In Fig. 8 all fractions up to denominator $t = 5$ were kept. One easily sees that one goes from one level to the other in the Farey tree thanks to the simple rule $\frac{0}{1} < \dots < \frac{p}{q} < \frac{p+p'}{q+q'} < \frac{p'}{q'} < \dots < \frac{1}{1}$, that is by adding numerators and denominators of adjacent fractions.

To compute the number of such fractions, one uses Euler function $\phi(n)$ which is defined as the number of integers less or equal to n and prime to it

$n :$	1	2	3	4	5	6	7	8	9	10	11	12...
$\phi(n) :$	1	1	2	2	4	2	6	4	6	4	10	4...

For example for $t = 5$, the irreducible fractions are $\frac{1}{5}, \frac{2}{5}, \frac{3}{5}, \frac{4}{5}$, that is $\phi(5) = 4$, where $q = 5$ is prime. If $t = 6$, the irreducible fractions are $\frac{1}{6}$ and $\frac{5}{6}$ so that $\phi(6) = 2$.

Fractions in the Farey tree have an arbitrary denominator less than or equal to t so that the whole number is

$$N = \Phi(t) = \sum_{n=1}^{n=t} \phi(n) \simeq \frac{3}{\pi^2} t^2 \tag{24}$$

The Farey tree decomposition leads to another important property which is still equivalent to Riemann hypothesis

$$\frac{|M(t)|}{2\pi} = \sum_{i=1}^{i=N} \delta_i = O(t^{\frac{1}{2}+\epsilon}) \quad \text{with} \quad \delta_i = \left| \frac{i}{N} - \frac{p_i}{q_i} \right| \tag{25}$$

The shift δ_i represented in Fig. 9 is the so-called Franel-Landau shift. It measures the position of the i^{th} Farey fraction versus the corresponding point in the equally spaced graduation. It looks very similar to the amplitude of the signal at the output of detector “D” [2]. One can thus expect that Riemann’s hypothesis may be hidden behind physical properties of “D” reported in the previous section.

Rather than the Möbius program let us now consider that the instantaneous phase at the receiver is given from the von Mangoldt function

$$\Lambda(n) = \begin{cases} \ln p & \text{if } n = p^k \text{ and } p \text{ prime} \\ 0 & \text{otherwise} \end{cases} \tag{26}$$

For example $\Lambda(2) = \ln 2$, $\Lambda(2^2) = \ln(2)$, $\Lambda(5) = \ln(5)$, $\Lambda(6) = 0$, ... At time t the cumulative phase jump is

$$\psi(t) = \sum_{n=1}^{n=t} \Lambda(n) = t + \epsilon(t) \tag{27}$$

In contrast to the “brownian type particle” in (21), one gets an “inertial” type motion plus a fluctuating term. It is most remarkable that the last term can be

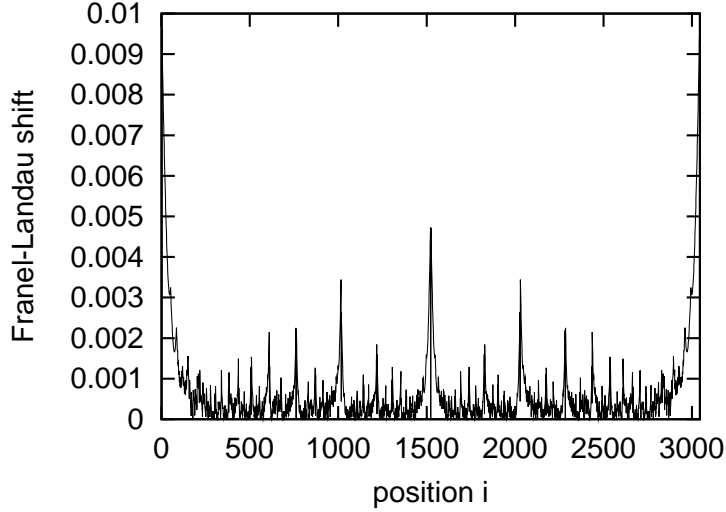


Fig 9. The Franel-Landau shift δ_i for $t = 100$ so that $N = 3045$

expressed analytically as [7]

$$\epsilon(t) = -\ln(2\pi) - \frac{1}{2} \ln(1 - t^{-2}) - \sum_{\rho} \frac{t^{\rho}}{\rho} \quad (28)$$

In (28) the three contributions correspond to singularities of the Riemann zeta function $\zeta(s)$, a function of the complex variable s introduced by Riemann in his famous paper on prime number theory [7]. Fig. 10 shows the mean frequency deviation $\frac{\epsilon(t)}{t} = \frac{\psi(t)}{t} - 1$ versus time t . Under Riemann hypothesis one gets this deviation bounded from the asymptotic expression

$$\frac{\epsilon(t)}{t} = O\left(\frac{\ln^2 t}{\sqrt{t}}\right) \quad (29)$$

In our approach randomness occurs through properties of prime numbers as sampled from two generic models: Möbius program (21) and von Mangoldt program (26). The asymptotic dependance of cumulative jumps is known thanks to Riemann hypothesis, a cornerstone of modern mathematics. The theory is quite intricate. We remind here the starting point and some connexions.

Riemann zeta function $\zeta(s)$ is defined from the Euler product

$$\zeta(s) = \sum_{n=1}^{\infty} \frac{1}{n^s} = \prod_{p \text{ prime}} \frac{1}{1 - \frac{1}{p^s}} \quad \text{where } \Re(s) > 1 \quad (30)$$

Riemann great achievement in 1859 was his ability to complete the formula to the whole complex plane of the variable s . Möbius function $\mu(n)$ and von Mangoldt function $\Lambda(n)$ connect to $\zeta(s)$ thanks to the expressions

$$\zeta_{\mu}(s) = \sum_{n=1}^{\infty} \frac{\mu(n)}{n^s} = \frac{1}{\zeta(s)} \quad (31)$$

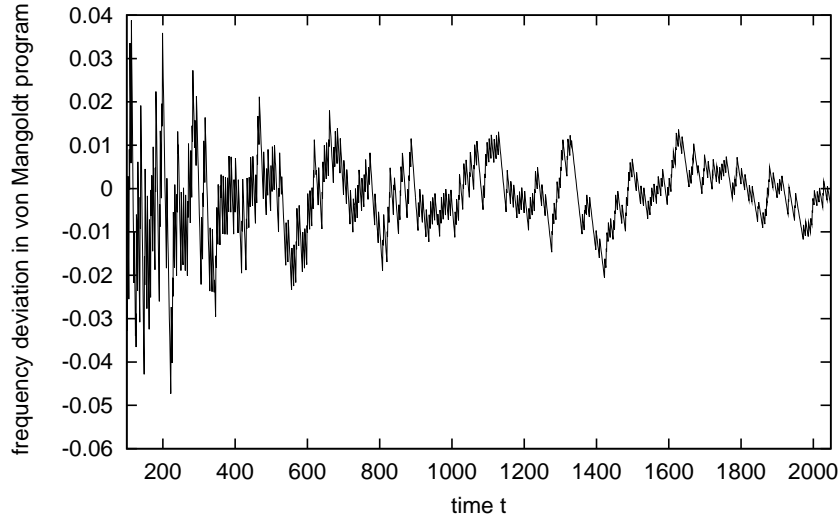


Fig 10. Mean frequency deviation for the von Mangoldt jumps

$$\zeta_{\Lambda}(s) = \sum_{n=1}^{\infty} \frac{\Lambda(n)}{n^s} = -\frac{\zeta'(s)}{\zeta(s)} = \frac{d}{ds}[\ln \zeta_{\mu}(s)] \quad (32)$$

The zeros of $\zeta(s)$ lead to poles in the inverse zeta function and its logarithmic derivative, and thus play a major role in the sums (22) and (27). From the completed zeta function [7] it is easy to find that they are (trivial) zeros on the negative real axis located at $s = -2l$ (l integer): they are responsible for the second term at the right hand side of (28). The remaining zeros of $\zeta(s)$ (billions of them have been computed) are located on the critical line $s = \frac{1}{2}$. Riemann hypothesis is the conjecture that all non trivial zeros are located on the critical line. These zeros are responsible for the third (random) term at the right hand side of (28).

One understands from now that randomness of the prime number distribution is reflected into the randomness of the position of zeros of $\zeta(s)$ on the critical line $s = \frac{1}{2}$. Another important result is that under Riemann hypothesis $\zeta_{\mu}(s)$ and $\zeta_{\Lambda}(s)$ are defined for $\Re(s) > \frac{1}{2}$.

On a physical point of view one can observe that n^s is a power law and $\zeta_{\mu}(s)$ and $\zeta_{\Lambda}(s)$ are measures with a critical exponent at $s = \frac{1}{2}$. In some respect the arithmetical approach supersedes the fractal point of view. See also the link between fractal geometry and number theory in the review by Lapidus [8].

We now want to emphasize the link to $1/F$ noise. We calculated numerically the power spectral density FFT of frequency fluctuations in von Mangoldt program

$$S(F) = \text{FFT}\left(\frac{\epsilon(t)}{t}\right) \quad (33)$$

As shown in Fig. 12 we observe that the fluctuations follow the condition

$$S(F) \times F \leq A \quad (34)$$

where A is constant and F is the Fourier frequency. This condition is typical of $1/F$ noise.

The connexion between prime number theory and physics is an emerging and fascinating field. A review of some theoretical links can be seen at the address <http://www.maths.ex.ac.uk/~mwatkins/zeta/physics.htm>

Self similarity in the distribution of primes was already evoked by M. Wolf [9]. In the present paper it is suggested from number theory that the randomness of time resets in the communication receiver “D” may resort to primes. However the connexion still needs to be refined before $1/F$ frequency noise in oscillators may be considered as a solved problem.

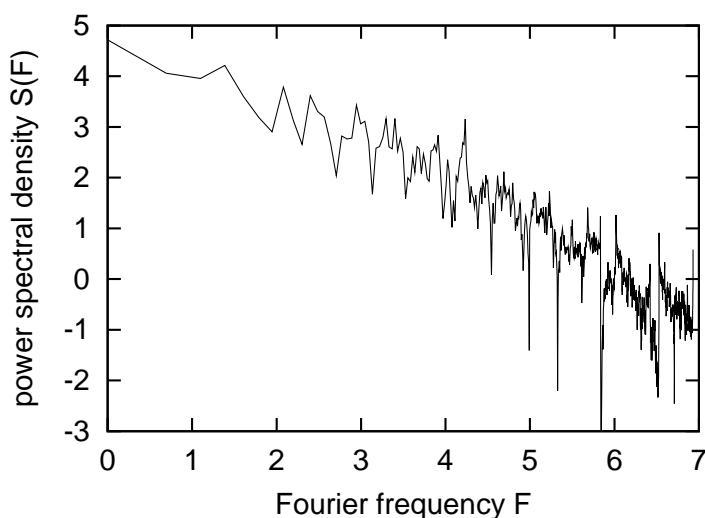


Fig 11. Power spectral density of frequency fluctuations in von Mangoldt program.

References

- [1] M. Planat, *Noise, Oscillators and Algebraic Randomness: from Noise in Communication Systems to Number Theory, Lecture Notes in Physics* **550**, Springer, Berlin (2000).
- [2] M. Planat and C. Eckert, *On the Frequency and Amplitude Spectrum and the Fluctuations at the Output of a Communication Receiver, IEEE Trans. on Ultrason. Ferroel. and Freq. Cont.* **47** (2000) 1173–1182.
- [3] S. Dos Santos and M. Planat, *Arithmetical fractals in an electronic loop*, in *Fractals and Beyond, Complexity and Fractals in the Sciences*, ed. M.N. Novak, World Scientific, Singapore (1998) 297–306.
- [4] J.R. Smith, *Modern Communication Circuits, Second Edition*. McGraw-Hill, Boston (1997)
- [5] M.R. Schroeder, *Number Theory in Science and Communication, Third Edition*, Springer, Berlin (1999).
- [6] J. Cresson and M. Planat, *Number Theory and Oscillators*, submitted to *Communication in Mathematical Physics*.

- [7] H.M. Edwards, *Riemann's zeta function*. Academic Press, New York (1974).
- [8] M.L. Lapidus and M. van Frankenhuysen, *Fractal Geometry and Number Theory*. Birkhäuser, Boston (1999).
- [9] M. Wolf, *1/f noise in the distribution of prime numbers*, *Physica A* **241** (1997) 493–499.